

Observers Design For Sensorless PMSMs

AHMED CHOUYA

Department of Genie Electrical
University of Djilali Bounaama
Khemis-Miliana City, 44 225
ALGERIA

Abstract: A state observer is proposed for permanent magnet synchronous motors (PMSMs). The gain of this observer involves a design function that has to satisfy some mild conditions which are given. Different expressions of such a function are proposed. Of particular interest, it is shown that high gain observers and sliding mode like observers can be derived by considering particular expressions of the design function. The simulation is given in order to compare the performance of a high gain observer and a sliding mode observer obtained through two different choices of the design function. Simulation is made by the software MATLAB/SIMULINK.

Key-Words: permanent magnet synchronous motors, high gain observer, sliding mode observer

Received: April 9, 2022. Revised: December 26, 2022. Accepted: January 18, 2023. Published: February 28, 2023.

1 Synchronous PMSM Model

Because of mechanical rotor position is practically unavailable for measurement devices, the PMSM model is considered in the $(\alpha - \beta)$ -frame which is more suitable for observer design. According to [1, 2], the PMSM model in the $(\alpha - \beta)$ coordinates is given by:

$$\begin{aligned} \frac{di_s}{dt} &= -\frac{R_s}{L_s}i_s - \frac{p}{L_s}\Omega\mathcal{J}_2\psi_r + \frac{1}{L_s}u \\ \frac{d\psi_r}{dt} &= p\Omega\mathcal{J}_2\psi_r \\ \frac{d\Omega}{dt} &= \frac{p}{J}i_s^T\mathcal{J}_2\psi_r - \frac{f_v}{J}\Omega - \frac{1}{J}T_l \\ \frac{dT_l}{dt} &= 0 \end{aligned} \quad (1)$$

Where $i_s = [i_{s\alpha} \ i_{s\beta}]^T$, $\psi_r = [\psi_{r\beta} \ \psi_{r\alpha}]^T$, $u = [u_{s\alpha} \ u_{s\beta}]^T$ are respectively, the stator currents, the rotor fluxes and the voltages. Ω and T_l respectively, denote the rotor speed and the load torque. \mathcal{J}_2 is the (2×2) matrix define as $\mathcal{J}_2 = \begin{bmatrix} 0 & -1 \\ 1 & 0 \end{bmatrix}$; J is the motor moment of inertia; p is the number of pairs of poles. The electrical parameters R_s and L_s are the stator resistor and inductance, respectively. Notice that the time derivative of the external load torque is described by an unknown bounded function. The first issue one must deal with is, under what conditions that all the state variables, i_s , ψ_r , Ω and T_l can be determined using only measurements of the electrical variables i.e. the stator current and supply voltage measurements i_s and u , respectively.

2 Model Transformation

For clarity our purposes, one introduces the following notations:

$$\begin{aligned} x &= \begin{bmatrix} x_1 \\ x_2 \\ x_3 \end{bmatrix} \quad \text{with } x_1 = \begin{bmatrix} x_{11} \\ x_{12} \end{bmatrix}, \quad x_2 = \begin{bmatrix} x_{21} \\ x_{22} \end{bmatrix}, \\ x_3 &= \begin{bmatrix} x_{31} \\ x_{32} \end{bmatrix}, \quad x_{11} = i_{s\alpha}, \quad x_{12} = i_{s\beta}, \\ x_{21} &= \psi_{r\alpha}, \quad x_{22} = \psi_{r\beta}, \quad x_{31} = \Omega, \quad x_{32} = T_l. \end{aligned} \quad (2)$$

In the sequel, the notation I_k and 0_k will be used to denote the $(k \times k)$ identity matrix and the $(k \times k)$ null matrix, respectively. The rectangular $(k \times m)$ null matrix shall be denoted by $0_{k \times m}$. Model (1) can then be rewritten under the following condensed form:

$$\begin{cases} \dot{x} &= f(x, u) \\ y &= Cx = x_1 \end{cases} \quad (3)$$

Where

$$\begin{aligned} f(x, u) &= \begin{bmatrix} f_1(x, u) \\ f_2(x, u) \\ f_3(x, u) \end{bmatrix} \\ &= \begin{bmatrix} -\frac{R_s}{L_s}x_1 - \frac{p}{L_s}x_{31}\mathcal{J}_2x_2 + \frac{1}{L_s}u \\ px_{31}\mathcal{J}_2x_2 \\ \left[\begin{array}{c} \frac{p}{J}x_1^T\mathcal{J}_2x_2 - \frac{f_v}{J}x_{31} - \frac{1}{J}x_{32} \\ 0 \end{array} \right] \end{bmatrix} \end{aligned}$$

$$C = [I_2 \quad 0_2 \quad 0_2] .$$

We need to transform system (3) to the triangular form.

One will introduce the change of variable according to :

$$\begin{cases} x_1 = x_1 \\ x_2 = x_{31} \mathcal{J}_2 x_2 \Rightarrow \dot{x}_2 = p x_2 \\ x_3 = x_3 \end{cases} \quad (4)$$

Then

$$\begin{cases} \dot{x} = f(x, u) \\ y = Cx = x_1 \end{cases} \quad (5)$$

Where

$$\begin{aligned} f(x, u) &= \begin{bmatrix} f_1(x_1, x_2, u) \\ f_2(x_1, x_2, x_3, u) \\ f_3(x, u) \end{bmatrix} \\ &= \begin{bmatrix} -\frac{R_s}{L_s} x_1 - \frac{p}{L_s} x_2 + \frac{1}{L_s} u \\ \frac{p}{J} x_1^T \mathcal{J}_2 x_2 \mathcal{J}_2 x_2 - \frac{f_v}{J} x_2 + \mathcal{J}_2 \begin{bmatrix} p x_2 \\ -\frac{1}{J} x_2 \end{bmatrix}^T x_3 \\ \begin{bmatrix} \frac{p}{J} x_1^T \mathcal{J}_2 x_2 - \frac{f_v}{J} x_{31} - \frac{1}{J} x_{32} \\ 0 \end{bmatrix} \end{bmatrix} \end{aligned}$$

and

$$C = [\mathcal{I}_2 \quad 0_2 \quad 0_2] .$$

We will introduce a classical state transformation. $\Phi \in \mathbb{R}^{6 \times 6}$ that puts model (1) under a known observable canonical form [3].

The sufficient conditions under which the considered state transformation is a diffeomorphism. In particular, this the analysis will emphasize the JACOBIAN matrix (of the considered state transformation) that is required to be full rank. Now, let us consider the following change of variables.

$$\begin{aligned} \Phi : \mathbb{R}^6 &\rightarrow \mathbb{R}^6 \\ x &\rightarrow z = \begin{bmatrix} z_1 \\ z_2 \\ z_3 \end{bmatrix} = \Phi(x) = \begin{bmatrix} \Phi_1(x) \\ \Phi_2(x) \\ \Phi_3(x) \end{bmatrix} \end{aligned} \quad (6)$$

$$\Phi(x) = \begin{bmatrix} x_1 \\ f_1(x_1, x_2, u) \\ \frac{\partial f_1(x_1, x_2, u)}{\partial x_2} f_2(x_1, x_2, x_3) \end{bmatrix}$$

The map Φ is one to one. Let Φ^{-1} denote its converse. Before deriving the dynamics of z , let us introduce the following notations :

$\Lambda(x, u)$ is the diagonal matrix :

$$\begin{aligned} \Lambda(x, u) &= \text{diag} \left(\mathcal{I}_2, \frac{\partial f_1(x_1, x_2, u)}{\partial x_2}, \right. \\ &\quad \left. \frac{\partial f_1(x_1, x_2, u)}{\partial x_2} \frac{\partial f_2(x_1, x_2, x_3)}{\partial x_3} \right) \\ &= \text{diag} \left(\mathcal{I}_2, -\frac{p}{L_s} \mathcal{I}_2, -\frac{p}{L_s} \mathcal{J}_2 \begin{bmatrix} p x_2 \\ -\frac{1}{J} x_2 \end{bmatrix}^T \right) \end{aligned} \quad (7)$$

$\Lambda(x, u)$ is left invertible. One shall denote by $\Lambda^{-1}(x, u)$ its left inverse. Now, one can easily check that :

$$\Lambda(x, u) f(x, u) = \mathcal{A}z + \varphi(z, u)$$

One can illustrate that the above state transformation puts system (5) under the following canonical form:

$$\begin{cases} \dot{z}_1 = z_2 + \varphi_1(z_1, u) \\ \dot{z}_2 = z_3 + \varphi_2(z_1, z_2) \\ \dot{z}_3 = \varphi_3(z) \\ y = Cz = z_1 \end{cases} \quad (8)$$

Where $z = [z_1 \quad z_2 \quad z_3]^T$; $z_k = [z_{k1} \quad z_{k2}]^T$ and $\varphi_k \in \mathbb{R}^2$, with $k = 1, 2, 3$;

3 Structure of Observer

For convenience, the system model (3) is given the following more compact form :

$$\begin{cases} \dot{z} = \mathcal{A}z + \varphi(z, u) \\ y = Cz = z_1 \end{cases} \quad (9)$$

where the state $z = [z_1 \quad z_2 \quad z_3]^T \in \mathbb{R}^6$, the matrix \mathcal{A} is the following anti-shift block matrix:

$$\mathcal{A} = \begin{bmatrix} 0_2 & \mathcal{I}_2 & 0_2 \\ 0_2 & 0_2 & \mathcal{I}_2 \\ 0_2 & 0_2 & 0_2 \end{bmatrix}$$

The function $\varphi(z, u)$ has a triangular structure :

$$\varphi(z, u) = \begin{pmatrix} \varphi_1(z_1, u) \\ \varphi_2(z_1, z_2) \\ \varphi_3(z) \end{pmatrix} \in \mathbb{R}^6$$

As in the works related to the observers synthesis [5, 6, 7, 8], one pose the hypothesis :

$\mathcal{H}1$: The function $\varphi(u, z)$ is globally Lipschitz with respect to z uniformly in u .

Before giving our candidate observers, one introduces the following notations.

1) Let Δ_θ is a block diagonal matrix define by:

$$\Delta_\theta = \text{diag} \left(\mathcal{I}_2, \frac{1}{\theta} \mathcal{I}_2, \frac{1}{\theta^2} \mathcal{I}_2 \right); \quad \theta > 0 \quad (10)$$

θ is a real number.

2) Let $S = S_{\theta=1}$ is a definit positive solution of the algebraic Lyapunov equation:

$$S + A^T S + S A - C^T C = 0 \quad (11)$$

Note that (11) is independent of the system and the solution can be expressed analytically. For a straightforward computation, its stationary solution is given by: $S_{(n,p)} = (-1)^{n+p} C_{n+p-2}^{n-1}$ where $C_n^p = \frac{n!}{p!(n-p)!}$

for $n \geq 1$ and $p \leq 3$; and then we can explicitly determine the correction gain of (3) as follows:

$$\theta \Lambda^{-1} \Delta_{\theta}^{-1} S^{-1} C^T = \begin{bmatrix} 3\theta \mathcal{I}_2 \\ -3 \frac{L_s}{p} \theta^2 \mathcal{I}_2 \\ -\frac{L_s}{p} \begin{bmatrix} p x_2 & -\frac{1}{J} x_2 \end{bmatrix}^{-1} \theta^3 \mathcal{I}_2 \end{bmatrix} \quad (12)$$

3) $\forall \xi = \begin{bmatrix} \xi_1 \\ \xi_2 \end{bmatrix}$, set $\bar{\xi} = \Delta_{\theta} \xi$ and let $\Upsilon(\xi) = \begin{bmatrix} \Upsilon_1(\xi_1) \\ \Upsilon_2(\xi_2) \end{bmatrix}$ be a vector of smooth functions satisfying:

$$\forall \xi \in \mathbb{R}^2 : \bar{\xi}^T \Upsilon(\xi) \geq \frac{1}{2} \xi^T C^T C \xi \quad (13)$$

$$\exists \kappa > 0; \forall \xi \in \mathbb{R}^2 : \|\Upsilon(\xi)\| \leq \kappa \|\xi\| \quad (14)$$

The system

$$\begin{aligned} \dot{\hat{z}} &= \mathcal{A} \hat{z} + \varphi(u, \hat{z}) - \theta \Delta_{\theta}^{-1} S^{-1} \Upsilon(\hat{z}_1) \\ &\quad - \frac{\partial \Phi(u, x)}{\partial x} \left(\Lambda^{-1} - \left(\frac{\partial \Phi(u, x)}{\partial x} \right)^{-1} \right) \theta \Delta_{\theta}^{-1} S^{-1} \Upsilon(\hat{z}_1) \end{aligned} \quad (15)$$

is an observer for (9); Where $\tilde{z} = \hat{z} - z$ error in estimation; $\Upsilon(\tilde{z})$ satisfies conditions (13) and (14).

3.1 Stability Analysis of the Proposed Observer

Now, we present the stability analysis of the candidate observer (15), for that let use the error consider \tilde{z} , his derivative :

$$\begin{aligned} \dot{\tilde{z}} &= \mathcal{A} \tilde{z} - \theta \Delta_{\theta}^{-1} S^{-1} \Upsilon(\tilde{z}_1) + \varphi(u, \hat{z}) - \varphi(u, z) \\ &\quad - \Gamma(u, \hat{z}) \theta \Delta_{\theta}^{-1} S^{-1} \Upsilon(\tilde{z}_1) \end{aligned}$$

Where

$$\Gamma(u, \hat{z}) = \frac{\partial \Phi(u, x)}{\partial x} \left(\Lambda^{-1} - \left(\frac{\partial \Phi(u, x)}{\partial x} \right)^{-1} \right)$$

Notice that $\Gamma(u, \hat{z})$ is a lower triangular matrix with zeros on its main diagonal, one can easily deduce that $\Gamma(u, \hat{z})$ is bounded.

Now, one can easily check the following identities:

- $\theta \Delta_{\theta}^{-1} \mathcal{A} \Delta_{\theta} = \mathcal{A}$
- $C \Delta_{\theta} = C$
- $\tilde{z} = \Delta_{\theta} \tilde{z}$

One obtains :

$$\begin{aligned} \dot{\tilde{z}} &= \theta \mathcal{A} \tilde{z} + \Delta_{\theta} (\varphi(u, \hat{z}) - \varphi(u, z)) \\ &\quad - \theta \Delta_{\theta} \Gamma(u, \hat{z}) \Delta_{\theta}^{-1} S^{-1} \Upsilon(\tilde{z}_1) - \theta S^{-1} C^T C \Upsilon(\tilde{z}_1) \end{aligned} \quad (16)$$

To prove convergence, let us consider the following equation of Lyapunov $V(\tilde{z}) = \tilde{z}^T S \tilde{z}$. By calculating the derivative of V along the \tilde{z} trajectories, we obtain:

$$\begin{aligned} \dot{V} &= 2\tilde{z}^T S \dot{\tilde{z}} \\ &= 2\theta \tilde{z}^T S \mathcal{A} \tilde{z} - 2\theta \tilde{z}^T \Upsilon(\tilde{z}_1) \\ &\quad + 2\tilde{z}^T S \Delta_{\theta} (\varphi(u, \hat{z}) - \varphi(u, z)) \\ &\quad - 2\theta \tilde{z}^T S \Delta_{\theta} \Gamma(u, \hat{z}) \Delta_{\theta}^{-1} S^{-1} \Upsilon(\tilde{z}_1) \\ &= \theta \tilde{z}^T (-S + C^T C) \tilde{z} - 2\theta \tilde{z}^T \Upsilon(\tilde{z}_1) \\ &\quad + 2\tilde{z}^T S \Delta_{\theta} (\varphi(u, \hat{z}) - \varphi(u, z)) \\ &\quad - 2\theta \tilde{z}^T S \Delta_{\theta} \Gamma(u, \hat{z}) \Delta_{\theta}^{-1} S^{-1} \Upsilon(\tilde{z}_1) \\ &= -\theta V + \theta \tilde{z}^T C^T C \tilde{z} - 2\theta \tilde{z}^T \Upsilon(\tilde{z}_1) \\ &\quad + 2\tilde{z}^T S \Delta_{\theta} (\varphi(u, \hat{z}) - \varphi(u, z)) \\ &\quad - 2\theta \tilde{z}^T S \Delta_{\theta} \Gamma(u, \hat{z}) \Delta_{\theta}^{-1} S^{-1} \Upsilon(\tilde{z}_1) \end{aligned}$$

By taking account of the (11) and (13) the derivative of V becomes:

$$\begin{aligned} \dot{V} &= -\theta V + 2\theta \left(\frac{1}{2} \tilde{z}^T C^T C \tilde{z} - \tilde{z}^T \Upsilon(\tilde{z}_1) \right) \\ &\quad + 2\tilde{z}^T S \Delta_{\theta} (\varphi(u, \hat{z}) - \varphi(u, z)) \\ &\quad - 2\theta \tilde{z}^T S \Delta_{\theta} \Gamma(u, \hat{z}) \Delta_{\theta}^{-1} S^{-1} \Upsilon(\tilde{z}_1) \\ &\leq -\theta V + 2\tilde{z}^T S \Delta_{\theta} (\varphi(u, \hat{z}) - \varphi(u, z)) \\ &\quad - 2\theta \tilde{z}^T S \Delta_{\theta} \Gamma(u, \hat{z}) \Delta_{\theta}^{-1} S^{-1} \Upsilon(\tilde{z}_1) \end{aligned} \quad (17)$$

Now, assume that $\theta \geq 1$, then, because of the triangular structure and the Lipschitz assumption on φ , one can show that :

$$\|\Delta_{\theta} (\varphi(u, \hat{z}) - \varphi(u, z))\| \leq \zeta \|\tilde{z}\| \quad (18)$$

where ζ is a constant of Lipschitz. Similarly, according to hypothesis $\mathcal{H}1$.

Using inequalities (14) inequality (17) becomes:

$$\begin{aligned} \dot{V} &\leq -\theta V + 2\lambda_{\max}(S) \|\tilde{z}\| (\zeta \|\tilde{z}\| + \varrho \eta(S) \|\tilde{z}_1\|) \\ &\leq -(\theta - c_1) V \end{aligned}$$

where $c_1 = 2\eta^2(S)(\zeta + \varrho \eta(S))$ with $\lambda_{\min}(S)$ and $\lambda_{\max}(S)$ being respectively the smallest and the largest eigenvalues of S and $\eta(S) = \sqrt{\frac{\lambda_{\max}(S)}{\lambda_{\min}(S)}}$.

Now taking $\theta_0 = \max\{1, c_1\}$ and using the fact that for $\theta \geq 1$, $\|\tilde{z}\| \leq \|\tilde{z}\| \leq \theta^2 \|\tilde{z}\|$, one can show that for $\theta > \theta_0$, one has :

$$\|\tilde{z}\| \leq \theta^2 \eta(S) \exp \left[- \left(\frac{\theta - c_1}{2} \right) t \right] \|\tilde{z}(0)\|$$

It is easy to see that λ and μ_{θ} needed by the result 1 are: $\lambda = \eta(S)$ and $\mu_{\theta} = \frac{\theta - c_1}{2}$. This completes the proof.

3.2 Observers Equations in the Original Coordinates

Proceeding as in [5], one can show that observer (15) can be written in the original coordinates x as follows:

$$\dot{\hat{x}} = f(u, \hat{x}) - \theta \Lambda^{-1} \Delta_{\theta}^{-1} S^{-1} \Upsilon(\hat{x}_1 - x_1) \quad (19)$$

Some expressions of $\Upsilon(\hat{x}_1 - x_1) = \Upsilon(\tilde{x}_1)$ that satisfying conditions (13) and (14) shall be given in this section and the so-obtained observers are discussed. These expressions will be given in the new coordinates z in order to easily check conditions (13) and (14) as well as in the original coordinates x in order to easily recognize the structure of the resulting observers.

3.3 High Gain Observer

Consider the following expression of $\Upsilon(\tilde{\xi})$:

$$\Upsilon_{HG}(\tilde{x}) = C^T C \tilde{x} = C^T \tilde{x}_1 \quad (20)$$

One can easily check that expression (20) satisfies conditions (13) and (14). Replacing $\Upsilon(\tilde{x})$ by expression (20) in (15) gives rise to a high gain observer (see e.g. [5, 7, 10]):

$$\dot{\hat{x}} = f(u, \hat{x}) - \theta \Lambda^{-1} \Delta_{\theta}^{-1} S^{-1} C^T (\hat{x}_1 - x_1) \quad (21)$$

Or

$$\begin{cases} \dot{\hat{x}}_1 = -\frac{R_s}{L_s} x_1 - \frac{p}{L_s} x_2 + \frac{1}{L_s} u - 3\theta(\hat{x}_1 - x_1) \\ \dot{\hat{x}}_2 = \frac{p}{J} x_1^T J_2 x_2 J_2 x_2 - \frac{f_v}{J} x_2 + J_2 \begin{bmatrix} p x_2 \\ -\frac{1}{J} x_2 \end{bmatrix}^T \\ \dot{\hat{x}}_3 = \begin{bmatrix} \frac{p}{J} x_1^T J_2 x_2 - \frac{f_v}{J} x_{31} - \frac{1}{J} x_{32} \\ -\theta^3(\hat{x}_1 - x_1) \end{bmatrix} \end{cases} x_3 \quad (22)$$

Referring to (4), the rotor flux is governed by the following equations:

$$\hat{x}_2 = \hat{\psi}_r = \frac{J_2^{-1} \hat{x}_2}{\hat{x}_3} \quad (23)$$

3.4 Sliding Mode Observers

At first glance, the following vector seems to be a potential candidate for the expression of $\Upsilon(\tilde{x})$:

$$\Upsilon_{\text{sign}}(\tilde{x}) = C^T C \text{sign}(\tilde{x}) = C^T \text{sign}(\tilde{x}_1) \quad (24)$$

where sign is the usual sign function with $\text{sign}(\tilde{x}_1) = \begin{bmatrix} \text{sign}(\tilde{x}_{11}) \\ \text{sign}(\tilde{x}_{12}) \end{bmatrix}$; then:

$$\dot{\hat{x}} = f(u, \hat{x}) - \theta \Lambda^{-1} \Delta_{\theta}^{-1} S^{-1} C^T \text{sign}(\hat{x}_1 - x_1) \quad (25)$$

Or

$$\begin{cases} \dot{\hat{x}}_1 = -\frac{R_s}{L_s} x_1 - \frac{p}{L_s} x_2 + \frac{1}{L_s} u - 3\theta \text{sign}(\hat{x}_1 - x_1) \\ \dot{\hat{x}}_2 = \frac{p}{J} x_1^T J_2 x_2 J_2 x_2 - \frac{f_v}{J} x_2 + J_2 \begin{bmatrix} p x_2 \\ -\frac{1}{J} x_2 \end{bmatrix}^T \\ \dot{\hat{x}}_3 = \begin{bmatrix} \frac{p}{J} x_1^T J_2 x_2 - \frac{f_v}{J} x_{31} - \frac{1}{J} x_{32} \\ 0 \\ -\theta^3 \text{sign}(\hat{x}_1 - x_1) \end{bmatrix} \end{cases} x_3 \quad (26)$$

Indeed, condition (13) is trivially satisfied by (24). Similarly, for bounded input bounded output systems. However, expression (24) cannot be used due to the discontinuity of the sign function. Indeed, such discontinuity makes the stability problem not well posed since the LYAPUNOV method used throughout the proof is not valid. In order to overcome these difficulties one shall use continuous functions which have similar properties to those of the sign function. This approach is widely used when implementing sliding mode observers. Indeed, consider the following function:

3.4.1 tanh Function

$$\Upsilon_{\tanh}(\tilde{x}) = C^T C \tanh(\tilde{x}) = C^T \tanh(\tilde{x}_1) \quad (27)$$

where \tanh denotes the hyperbolic tangent function; then:

$$\dot{\hat{x}} = f(u, \hat{x}) - \theta \Lambda^{-1} \Delta_{\theta}^{-1} S^{-1} C^T \tanh(\hat{x}_1 - x_1) \quad (28)$$

Or

$$\begin{cases} \dot{\hat{x}}_1 = -\frac{R_s}{L_s} x_1 - \frac{p}{L_s} x_2 + \frac{1}{L_s} u - 3\theta \tanh(\hat{x}_1 - x_1) \\ \dot{\hat{x}}_2 = \frac{p}{J} x_1^T J_2 x_2 J_2 x_2 - \frac{f_v}{J} x_2 + J_2 \begin{bmatrix} p x_2 \\ -\frac{1}{J} x_2 \end{bmatrix}^T \\ \dot{\hat{x}}_3 = \begin{bmatrix} \frac{p}{J} x_1^T J_2 x_2 - \frac{f_v}{J} x_{31} - \frac{1}{J} x_{32} \\ 0 \\ -\theta^3 \tanh(\hat{x}_1 - x_1) \end{bmatrix} \end{cases} x_3 \quad (29)$$

3.4.2 arctan Function

$$\Upsilon_{\arctan}(\tilde{x}) = C^T C \arctan(\tilde{x}) = C^T \arctan(\tilde{x}_1) \quad (30)$$

Similarly to the hyperbolic tangent function, one can easily check that the inverse tangent function:

$$\dot{\hat{x}} = f(u, \hat{x}) - \theta \Lambda^{-1} \Delta_{\theta}^{-1} S^{-1} C^T \arctan(\hat{x}_1 - x_1) \quad (31)$$

Or

$$\begin{cases} \dot{\hat{x}}_1 = -\frac{R_s}{L_s}x_1 - \frac{p}{L_s}x_2 + \frac{1}{L_s}u - 3\theta \arctan(\hat{x}_1 - x_1) \\ \dot{\hat{x}}_2 = \frac{p}{J}x_1^T \mathcal{J}_2 x_2 \mathcal{J}_2 x_2 - \frac{f_v}{J}x_2 + \mathcal{J}_2 \begin{bmatrix} px_2 \\ -\frac{1}{J}x_2 \end{bmatrix}^T x_3 \\ \dot{\hat{x}}_3 = \begin{bmatrix} -3\theta^2 \arctan(\hat{x}_1 - x_1) \\ \frac{p}{J}x_1^T \mathcal{J}_2 x_2 - \frac{f_v}{J}x_{31} - \frac{1}{J}x_{32} \\ 0 \\ -\theta^3 \arctan(\hat{x}_1 - x_1) \end{bmatrix} \end{cases} \quad (32)$$

4 Comparison of Sensorless Observers

To examine practical usefulness, the proposed observer has been simulated for a PMSM (see [11, 12]), whose parameters are depicted in Table 1.

Table 1: PMSM parameters used in simulations.

| Parameters | Notation | Value | Unit |
|------------|--------------------------|------------------------|----------|
| p | Pairs number of poles | 2 | |
| f | Frequency | 50 | s^{-1} |
| L_s | Inductance | 0.02682 | H |
| Ψ_r | Flux linkage established | 0.1717 | $V.s$ |
| R_s | Stator phase resistance | 18.7 | Ω |
| f_v | Friction factor | 1.349×10^{-5} | $N.m.s$ |
| J | Inertia | 0.26×10^{-5} | $Kg.m^2$ |
| T_l | Torque | 0.5 | $N.m$ |

In order to evaluate the observer behaviour in the realistic situation, the measurements of x_1 issued from the model simulation have been corrupted by noise measurements with a zero mean value. The torque lead takes the step value.

4.1 High Gain Observer

The adjustment parameter of the observer (22) is to chosen $\theta = 5.2$. The dynamic behaviour of the error of rotor flu is depicted in Figure Fig.1 graph (a); when graph (b) shows the gaussian errors density and empirical errors histogram of rotor flu error. The means of error flu equal -13.1×10^{-3} with very small variance 2.7088×10^{-6} this is almost surety. The pace of speed error is given by the figur Fig.2 graph (a) and the gaussian errors density and empirical errors histogram of rotor speed error are presented in graph (b) where means of error rotating speed equal -2.57×10^{-2} and variance equal 7.9359; the curve of load torque is illustrated on figur Fig.3 graph (a). In

graph (b) appear gaussian errors density and empirical errors histogram of load torque error where means of error load torque equal 0.3559 and variance equal 0.13×10^{-2} .

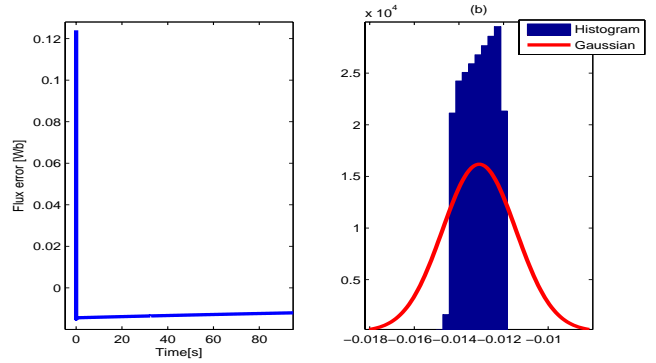


Figure 1: (a) Flux error. (b) Gaussian and histogram of error flux

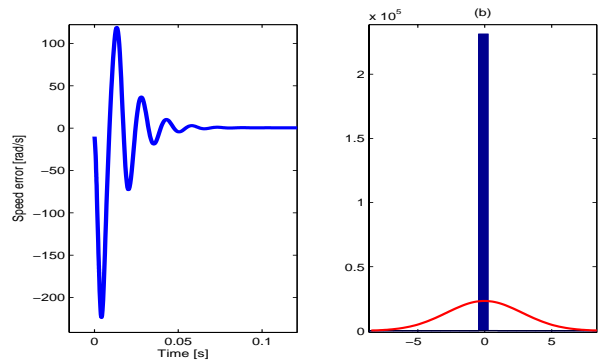


Figure 2: (a) Speed error. (b) Gaussian and histogram of error speed.

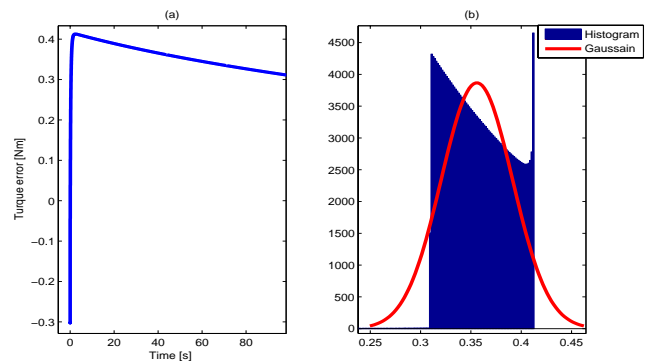


Figure 3: (a) Load torque error. (b) Gaussian and histogram of error load torque.

4.2 Sliding Mode Observer With tanh Function

Estimation results of the proposed algorithm (29) with $\theta = 4$ is reported in Figure Fig.4, Fig.5 and Fig.6. The behaviour of the error of rotor flu is depicted in fig Fig.4 graph (a); when graph (b) shows the gaussian errors density and empirical errors histogram of rotor flu error. The means of error flu equal 31.47×10^{-2} with very small variance 3.9×10^{-3} this is almost surety. The pace of speed error is given by the fig Fig.5 graph (a) and the gaussian errors density and empirical errors histogram of rotor speed error are presented in graph (b) where means of error rotating speed equal 6.5713 and variance equal 9.9518×10^3 ; the curve of load torque is illustrated on fig Fig.6 graph (a). In graph (b) appear gaussian errors density and empirical errors histogram of load torque error where means of error load torque equal -0.6595 and variance equal 0.0093

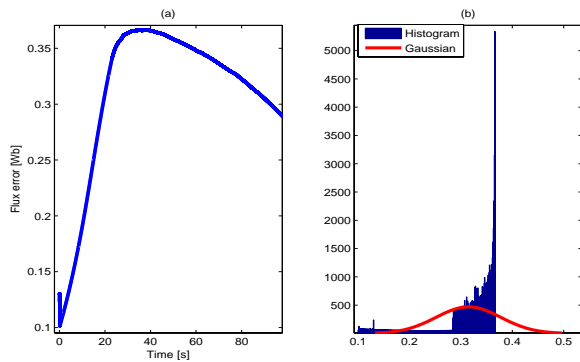


Figure 4: (a) Flux error. (b) Gaussian and histogram of error flux

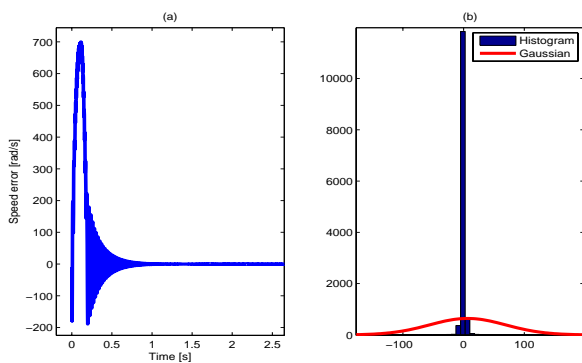


Figure 5: (a) Speed error. (b) Gaussian and histogram of error speed.

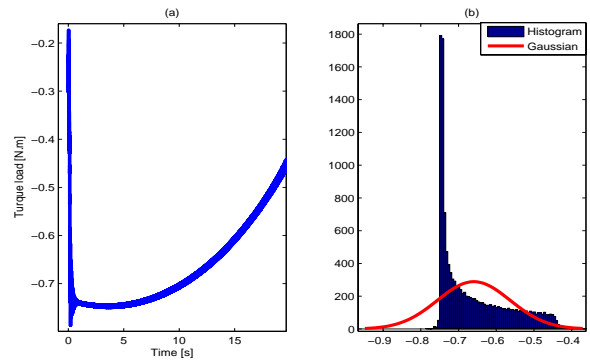


Figure 6: (a) Load torque error. (b) Gaussian and histogram of error load torque.

4.3 Sliding Mode Observer arctan Function

Under the same conditions with the function tanh. One simulates for the function arctan. The fig Fig.7, Fig.8 and Fig.9 illustrates the pace of error flux error speed and error load torque in respectively. The behaviour of the error of rotor flu is depicted in Figure Fig.7 graph (a); when graph (b) shows the gaussian errors density and empirical errors histogram of rotor flu error. The means of error flu equal 16.80×10^{-2} with very small variance 5.3206×10^{-3} this is almost surety. The pace of speed error is given by the fig Fig.8 graph (a) and the gaussian errors density and empirical errors histogram of rotor speed error are presented in graph (b) where means of error rotating speed equal 8.9159 and variance equal 5.336×10^3 ; the curve of load torque is illustrated on fig Fig.9 graph (a). In graph (b) appear gaussian errors density and empirical errors histogram of load torque error where means of error load torque equal -0.7050 and variance equal 0.0037

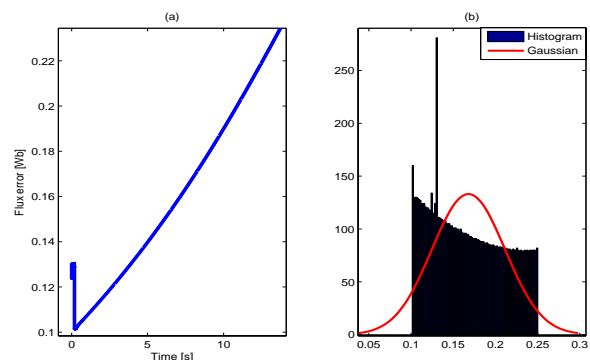


Figure 7: (a) Flux error. (b) Gaussian and histogram of error flux

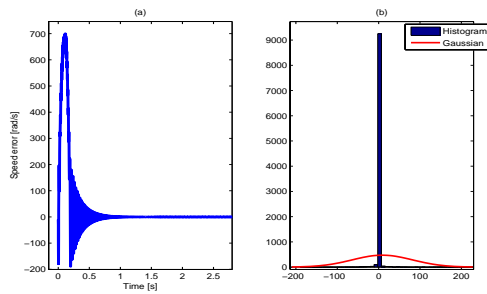


Figure 8: (a) Speed error. (b) Gaussian and histogram of error speed.

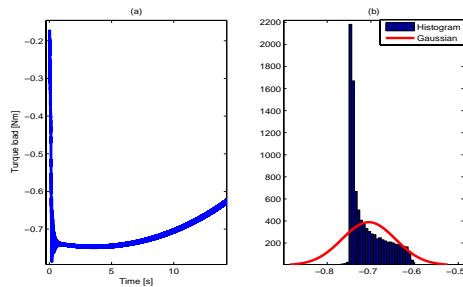


Figure 9: (a) Load torque error. (b) Gaussian and histogram of error load torque.

5 Conclusions

In this paper, high gain and alternative form for a sliding mode observers are presented. they is observer makes possible to observe, rotor flux rotor speed and load torque. An observer with high gain and three others with sliding mode which the functions sign, tanh and arctan. Observer whose sign gives chattering. High gain observer is good for the observation of rotor flux rotating speed and load torque.

References:

- [1] A. El magri , F. Giri and A. El Fadili. AC Electric Motors Control: Advanced Design Techniques and Applications, chapter Control Models for Synchronous Machines, 4156. Wiley, Oxford.doi:10.1002/9781118574263.ch3.
- [2] A.A.R.Al Tahir, A.El Magri, T. Ahmed-Ali, A. El Fadili and F. Giri. Sampled-Data Nonlinear Observer Design for Sensorless Synchronous PMSM. IFAC-PapersOnLine 48-11 (2015) pp:327-332.
- [3] J. Gauthier and I.Kupka. Deterministic observation theory and applications. Cambridge University Press. 2001.
- [4] R. Hermann and A. Krener. Nonlinear controllability and observability. IEEE Transactions on Automatic Control, 22(5), pp:728740, 1977.
- [5] M. Farza, M. M'Saad and L. Rossignol. Observer design for a class of MIMO nonlinear systems. Automatica, vol.40, pp.135-143, 2004.

- [6] G. Bornard and H. Hammouri. A high gain observer for a class of uniformly observable systems. In: Proc. 30th IEEE Conference on Decision and Control, Vol. 122. Brighton, England, 1991.
- [7] J.P. Gauthier, H. Hammouri and S. Othman. A simple observer for nonlinear systems: application to bioreactors. IEEE Trans. on Aut. Control, vol.37, pp.875880, 1992.
- [8] Chouya Ahmed, Contribution à l'Observation de la Machine Asynchrone, Editions Universitaires Européennes, Publié le:18-4-2019, ISBN-13: 978-3-639-54522-7, ISBN-10: 3639545222, EAN: 9783639545227 <https://www.morebooks.de/store/gb/book/contributoin-%C3%80-l-observation-de-la-machine-asynchrone/isbn/978-3-639-54522-7>
- [9] M. Farza, M. M'Saad, M. Sekher, A set of observers for a class of nonlinear systems, in: 16th IFAC W. C., Czech R., 2005.
- [10] H. Hammouri, and M. Farza. Nonlinear observers for locally uniformly observable systems. ESAIM J. on Control, Optimisation and Calculus of Variations; vol.9, pp.353-370, 2003.
- [11] Simulink Library Browser; Block Parameters : Permanent Magnet Synchronous Machine; back EMF waveform: Sinusoidal; mechanical input: Torque Tm; Preset model: No.
- [12] Ahmed Chouya, Kada Boureguigue, Mohamed Chenafa, Abdellah Mansouri. Adaptive Field-Oriented Control for the Permanent Magnet Synchronous Machine . International Journal of Instrumentation and Measurement. ISSN: 2534-8841. Volume 4, 27 December 2019. pp.17-22 . <https://www.ias.org/ias/home/caijim/adaptive-field-oriented-control-fo-the-permanent-magnet-synchronous-machine>

Contribution of Individual Authors to the Creation of a Scientific Article (Ghostwriting Policy)

The author contributed in the present research, at all stages from the formulation of the problem to the final findings and solution.

Sources of Funding for Research Presented in a Scientific Article or Scientific Article Itself

No funding was received for conducting this study.

Conflict of Interest

The author has no conflict of interest to declare that is relevant to the content of this article.

Creative Commons Attribution License 4.0 (Attribution 4.0 International, CC BY 4.0)

This article is published under the terms of the Creative Commons Attribution License 4.0 https://creativecommons.org/licenses/by/4.0/deed.en_US